



Extratropical cyclone statistics during the last millennium and the 21st century

Christoph C. Raible^{1,2}, Martina Messmer^{1,2}, Flavio Lehner³, Thomas F. Stocker^{1,2}, and Richard Blender⁴

¹Climate and Environmental Physics, University of Bern, Bern, Switzerland

²Oeschger Centre for Climate Change Research, Bern, Switzerland

³National Center for Atmospheric Research, Boulder (CO), USA

⁴Meteorological Institute, University of Hamburg, Hamburg, Germany

Correspondence to: C. C. Raible Climate and Environmental Physics, University of Bern, Sidlerstrasse 5, 3012 Bern, Switzerland raible@climate.unibe.ch

Abstract. Extratropical cyclones in winter and their characteristics are investigated in depth for the Atlantic European region, as they are responsible for a significant part of the rainfall and extreme wind and/or precipitation-induced hazards. Here, we use a seamless transient simulation with a state-of-the-art fully-coupled Earth System Model from 850 to 2100 CE as basis for the analysis. The RCP8.5 scenario is applied in the 21st century. During the Common Era, cyclone characteristics show pronounced variations on interannual and decadal time scales, but no external forcing imprint is found prior to 1850. Thus, variations of extratropical cyclone characteristics are mainly caused by internal variability of the coupled climate system. When anthropogenic forcing becomes dominant in the 20th century, a decrease of the cyclone occurrences mainly over the Mediterranean and a strong increase of extreme cyclone-related precipitation become detectable. The latter is due to thermodynamics as it follows the Clausius-Clapeyron relation. An important finding, though, is that the relation between temperature and extreme cyclone-related precipitation is not always controlled by the Clausius-Clapeyron relation, which suggests that dynamical processes can play an important role in generating extreme cyclone-related precipitation - for example in the absence of anomalously warm background conditions. Thus, the importance of dynamical processes, even on decadal time scales, might explain the conundrum that proxy records suggest enhanced occurrence of precipitation extremes during rather cold periods in the past.



20 1 Introduction

Extratropical cyclones are fundamental phenomena of the day-to-day weather variability. Extreme extratropical cyclones have a strong impact on society and economy and are one of the major natural hazards of the mid-latitudes (e.g., Schiesser et al., 1997; Beniston, 2007; Etienne et al., 2013). Thus, a better understanding of variations of cyclone characteristics is essential and has led to a variety of studies which assess recent and future changes in cyclone characteristics (e.g., Ulbrich et al., 2008; Bengtsson et al., 2009; Pinto et al., 2009; Raible et al., 2010; Schneider et al., 2010; Zappa et al., 2013; IPCC, 2013). Still, considerable uncertainty remains of how extratropical cyclones react to changes of external forcing, especially in the 21st century (Harvey et al., 2012; IPCC, 2013) as confounding and partly canceling processes are difficult to disentangle (O’Gorman, 2010; Woollings et al., 2012b). Additionally, low-frequency internal variability might be important, e.g., a potential influence of the Atlantic Meridional Overturning Circulation (AMOC) on cyclones has been discussed (Woollings et al., 2012a, 2015). Some of the uncertainties also arise from the fact that the observed time period is rather short, making it difficult to validate model-simulated decadal variability in cyclone statistics. Further, there are only a few modelling studies which put changes of extratropical cyclone characteristics in a long-term perspective (Fischer-Bruns et al., 2005; Raible et al., 2007; Gagen et al., 2016). A possibility to overcome this is the last millennium which enables us to study the external forcing imprint on extratropical cyclone characteristics and the interaction of internal variability of the climate system with these characteristics (Bothe et al., 2015; Smerdon et al., 2017).

The purpose of this study is to establish a long-term, pre-instrumental perspective for cyclone characteristics. In particular, we evaluate the future of these characteristics under the RCP8.5 scenario and compare it to natural variability during the last millennium. We take advantage of a transient simulation for the last millennium in high resolution (approx. $1^\circ \times 1^\circ$) which provides 12-h output — a necessity to investigate extratropical cyclones and their characteristics, such as cyclone-associated wind and precipitation extremes. The focus of the analysis is on the North Atlantic region and winter (December to February).

Various studies have analyzed the climate change response of extratropical cyclones and some of their characteristics (e.g., Ulbrich et al., 2008; Zappa et al., 2013; IPCC, 2013). A robust finding is that the warmer atmosphere in the future leads to a moistening of extratropical cyclones and thus to more precipitation (Bengtsson et al., 2009; Zappa et al., 2013). In the North Atlantic, an extension of the storm track into Europe is suggested under future climate change (e.g., Bengtsson et al., 2006; Catto et al., 2011; McDonald, 2011; Zappa et al., 2013). Further modelling studies suggest that the wind intensity of extratropical cyclones in the North Atlantic is projected to be enhanced in the future compared to today, leading to a higher potential of future losses (Pinto et al., 2012). A process relevant for this intensification is a local minimum in the warming of the North Atlantic



Ocean due to a reduction of the AMOC (Rahmstorf et al., 2015). This temperature anomaly leads to stronger temperature gradients within the North Atlantic basin than today and thus to enhanced low-level baroclinicity (Laine et al., 2009; Catto et al., 2011; Woollings et al., 2012b).

Substantial uncertainty remains in future projections of extratropical cyclone characteristics because of the processes involved (Harvey et al., 2012). The decrease of the projected meridional temperature gradient on average (due to polar amplification) implies a decrease of storm activity in the future, but at the same time the vertical temperature gradient decreases over the Atlantic and Arctic, which induces a reduced static stability and thus a favoring of storm growth (Harvey et al., 2012). Additionally, the moisture changes also influence the cyclone formation as latent heating arising from moist condensation often strengthens cyclones due to diabatic potential vorticity anomalies (e.g., Gutowski et al., 1992; Li et al., 2014), such that one would expect an intensification of cyclones in a warmer, moister climate (Willison et al., 2013). However, increased moisture, and therefore latent heat content in the global circulation leads to a more efficient poleward transport of energy, and therefore to a weakening of cyclonic activity in the mid-latitudes (e.g., O’Gorman and Schneider, 2008; Schneider et al., 2010; Li et al., 2014). Additionally, other processes like changes in the wave-wave interaction (James and James, 1989; Riviere, 2011) and in the eddy length scale (Kidston et al., 2011) might play a role for the response of extratropical cyclones to future anthropogenic forcing changes and for the uncertainty of the response in different climate model simulations.

The past can serve as a test bed to place future projection of extratropical cyclone characteristics into context and to assess multi-decadal variability. Climate states completely different from the present, like the Last Glacial Maximum show pronounced differences in extratropical cyclone behavior. Hofer et al. (2012a,b) showed that cyclones tend to move more zonally over the North Atlantic leading to enhanced precipitation in Southern Europe in winter. The reason is a southward shift of the eddy driven jet due to the Laurentide ice sheet (Merz et al., 2015). However, in the last interglacial, the Eemian (130 ka ago), the jet positions and thus the cyclones are similar to present (Merz et al., 2015). More relevant is potentially the recent past, i.e., the last millennium including the Medieval Warm Period (approx. 11th to the 13th century) and the Little Ice Age (LIA, approx. 14th to the 19th century; e.g., Bradley and Jones, 1993; Broecker, 2000; McGregor et al., 2015), as these periods are precursors of the Anthropocene (Zalasiewicz et al., 2010) and, thus, provide a rich and highly resolved proxy network (e.g., PAGES 2k Consortium, 2013). In multi-century pre-industrial climate model simulations, Fischer-Bruns et al. (2005) suggested that natural variability of extratropical cyclones is unrelated to external forcing like total solar irradiance (TSI), or volcanoes. This is in contrast to the modelling study of Raible et al. (2007) who found a significant intensification of cyclones in the North Atlantic during the Maunder Minimum (a period of reduced TSI from AD 1640-1715) compared to today, although part of the signal is already of anthropogenic origin. They further showed that low-level baroclinicity is enhanced due to the increased meridional temperature gradient, which seems to be the dominant process for cyclone intensification in their



coarsely resolved simulations. Comparing this model result with proxy records shows that during the LIA more severe storms are observed (Björck and Clemmensen, 2004; de Jong et al., 2007; 95 Sabatier et al., 2012; Trouet et al., 2012; Van Vliet-Lanoe et al., 2014; Degeai et al., 2015; Costas et al., 2016).

Since the early attempts to assess past extratropical cyclone behavior in model simulations (e.g., Fischer-Bruns et al., 2005; Raible et al., 2007) the ability to perform millennium-size simulations in high resolution has improved so that today several simulations for the last millennium based on 100 different models are available (Schmidt et al., 2011; Braconnot et al., 2012; Taylor et al., 2012; Otto-Bliesner et al., 2016). Still, most of these simulations have only saved monthly data, which prevent us to analyze extratropical cyclones in these simulations. Recently, a last millennium simulation spanning the period AD 850 to 2099 became available providing 12-h data (Lehner et al., 2015). This enables us to address the following research questions:

- 105
- How are cyclone characteristics projected to change in the 21st century?
 - How do these changes compare with variability, in particular low-frequency variation, during the last millennium?

The study is structured as follows: Section 2 briefly presents the model and experimental design chosen to generate the last millennium simulation. Further, the cyclone detection and tracking method 110 is introduced and the cyclone characteristics are defined. In Section 3 the last millennium simulation is compared with ERA interim for the period AD 1980 to 2009 to demonstrate the model's ability in simulating cyclone characteristics. Then, the climate change signals of the different characteristics are put into context to the low-frequency variability (Section 4). Finally, the results are summarized and discussed and concluding remarks are presented in Section 5.

115 2 Model and methods

2.1 Model and experimental design

To investigate the characteristics of extratropical cyclones we use the Community Earth System Model (CESM, 1.0.1 release; Hurrell et al., 2013). It is a state-of-the-art fully-coupled Earth System Model developed by the National Center for Atmospheric Research. CESM relies on the Community 120 Climate System Model (CCSM; Gent et al., 2011) in terms of the model physics, but it contains a carbon cycle module, which is included in its atmosphere, land and ocean components.

The CESM is used in the so-called 1° version to simulate the entire last millennium from AD 850 to 2099. The finite volume core of the atmosphere has a uniform horizontal resolution of $1.25^\circ \times 0.9^\circ$ at 26 vertical levels. The initial conditions for this transient simulation are obtained from a 500-yr 125 control simulation for perpetual AD 850 conditions, which was run into a quasi-equilibrium state



(no drift of the global mean temperature in the upper part of the ocean). The transient external forcing follows the Paleo Model Intercomparison Project 3 (PMIP3) protocols (Schmidt et al., 2011) and the Coupled Model Intercomparison Project 5 (Taylor et al., 2012). It consists of TSI, volcanic and anthropogenic aerosols, land use change, and greenhouse gases (GHGs; Fig. 1). Note that the TSI deviates from the PMIP3 protocol in that the amplitude between the Maunder Minimum (1640-1715) and today is doubled. Further, the model has enabled the carbon cycle module. To extend the simulation beyond AD 2005 the RCP8.5 is applied, which corresponds to a radiative forcing of approximately 8.5 W m^{-2} by 2100. Further details on the simulation are summarized in Lehner et al. (2015).

The analysis is based on 12-h instantaneous output, a resolution sufficient to derive characteristics of extratropical cyclones. The analysis focuses on the North Atlantic region in winter (December to February, DJF).

2.2 Cyclone detection, tracking, and characteristics

The cyclone analysis is based on a modified Lagrangian cyclone detection and tracking scheme first developed by Blender et al. (1997). The method is applied to the 1000-hPa geopotential height field and consists of two steps: (i) cyclone detection and (ii) tracking:

(i) A low pressure system is identified as a minimum in the geopotential height at 1000 hPa in a neighborhood of eight grid points and its intensity (in gpm/1000 km) defined as the mean gradient between the local geopotential height minimum and its neighboring grid points within an area of 1000 km distance to the minimum. To neglect weak or unrealistic minima, a minimum threshold value of this intensity measure is set to 20 gpm/1000 km. Further, cyclone centers identified in high topography (above 1000 m a.s.l.) are excluded.

(ii) To connect identified pressure minima a next neighborhood search is applied within a search radius of 1000 km. To further prevent erroneous detection of cyclones, two additional thresholds are used: the cyclone has a minimum lifetime of 24 hours, and the intensity (defined above) needs to exceed 30 gpm/1000 km once in its lifetime. More details on the cyclone detection algorithm are provided in Blender et al. (1997), Raible and Blender (2004) and Raible (2007). Furthermore, an intercomparison of different cyclone detection and tracking methods showed that the method used in this study is within the range of other methods (Raible et al., 2008; Neu et al., 2013). In particular, the agreement between the methods increases when focusing on extreme cyclones (Neu et al., 2013; Lionello et al., 2016; Grieger et al., 2018).

The Lagrangian cyclone detection and tracking method provides a variety of extratropical cyclone characteristics. Besides the number of time steps when a cyclone is present (or cumulative cyclone presence), intensity measures for wind are deduced, i.e., the central sea level pressure and the cyclone depth. The latter is the difference between the central geopotential height and the surrounding mean



geopotential height in distance of the radius of the cyclone (defined below). The 90th percentile of central pressure and cyclone depth of all cyclones within a season is used to define extremeness of wind related measures.

165 The radius is estimated by a Gaussian radius-depth method based on Schneidereit et al. (2010) to estimate the geometric structure of the cyclones. Thereby, the geopotential height surface in the neighborhood of a cyclone minimum is approximated by a Gaussian, which is fitted by a least squares method. The standard deviation of the Gaussian is then an estimation of the cyclone radius, another characteristic of extratropical cyclones.

170 Further, the area of the cyclone defined by this radius is used to quantify the amount of precipitation, related to this cyclone. The precipitation is integrated over this area for each time step of the cyclone and defines the cyclone-specific precipitation. To focus on extreme cyclone-specific precipitation, the 90th percentile of cyclone-related precipitation estimated within the season is used as an index of extremeness. A similar approach is selected to deduce cyclone-related temperature, though for this index we are interested in the mean of the season and not in the 90th percentile.

175 The radius is also used to deduce the Eulerian measure of cyclone occurrences, the so-called cyclone frequency. For one time step each grid point within the radius of a cyclone is assigned to be occupied by the cyclone. Summing over all time steps for each grid point and dividing by the total number of time steps results in cyclone frequency at each grid point. This measure enables us to identify regions of high and low cyclone occurrence.

180 All extratropical cyclone characteristics mentioned above are deduced for the North Atlantic region defined as $30^{\circ} - 70^{\circ}\text{N}$ and $65^{\circ}\text{W} - 40^{\circ}\text{E}$ (Fig. 2a).

3 Model evaluation

Before extratropical cyclone characteristics for the last millennium and the future are presented, the model's ability to simulate cyclones is demonstrated for the period CE 1980–2009 for winter (DJF).

185 To compare the simulated cyclones and their characteristics the ERA interim reanalysis data are used (Dee et al., 2011). The ERA interim data are first bi-linearly interpolated to the same resolution as CESM ($1.25^{\circ} \times 0.9^{\circ}$).

190 Figure 2 shows the cyclone frequency of the CESM simulation and ERA interim. The main centers of enhanced cyclone occurrence are realistically simulated, i.e., cyclone genesis region over Northern America, the North Atlantic storm track, as well as the Island low pressure region. Still, the CESM tends to simulate more cyclones over the North Atlantic compared to ERA interim. Some differences are found around Greenland and the Hudson Bay where CESM overestimates the cyclone frequency. The reason for this is partly the fact that geopotential height over orography is extrapolated to 1000 hPa leading to artificial high pressure and thus a tendency to weak low pres-



195 sure systems in the surrounding ocean regions. Still, most of the cyclones in the Labrador Sea are
cyclones originating from the cyclone genesis area around Newfoundland. Another caveat is visible
over the Mediterranean where CESM slightly underestimates cyclones over the western and central
Mediterranean and overestimates cyclone occurrence in the eastern part. Thus, the interpretation of
the results over polar regions around Greenland and the Mediterranean requires particular caution.

200 To further assess the model's ability in extratropical cyclone simulation, distributions of different
cyclone characteristics are presented in Fig. 3. We focus on the area North Atlantic marked in
Fig. 2a. In total 12369 cyclones are identified in CESM and 7624 in ERA interim. The life time of
the cyclones show a similar distribution for CESM and ERA interim (Fig. 3a). CESM shows a
slight overestimation of short-lived cyclones and underestimates long-lived cyclones (> 48 h). This
205 is a first hint that more weak cyclones are identified in CESM compared to ERA interim explaining
partly the higher cyclone frequencies (Fig. 2). The results of the radius confirm this finding as CESM
tends to underestimate the radius, still the shape of the distribution agrees with ERA interim. The
wind-sensitive measures show an interesting behavior. Although the shape agrees between CESM
and ERA interim, CESM shows more wind intensive cyclones when considering the measure cy-
210 clone depth. The central SLP measure shows a similar behavior with lower central SLP for CESM
than for ERA interim, but also the cumulative cyclone presence with high central SLP is increased
in CESM compared to ERA interim. Again the latter indicates that weak cyclones lead to higher
cyclone frequencies (Fig. 2). The cyclone-related precipitation shows that CESM slightly underesti-
mates precipitation except for extreme precipitation events (> 17 mm/day).

215 Besides the distributions, the model should also be able to simulate interannual connections between
the indices (if they exist). To uncover such connections, the cumulative cyclone presence, median of
the cyclone radius and the 90th percentile of cyclone depth, SLP and cyclone-related precipitation
in each winter season are estimated and the resulting time series are considered. Table 1 summa-
rizes pairwise correlations for these quantities derived from CESM and ERA interim, respectively.

220 Significant correlations (5 % significance level) are found between the two wind-related intensity
measures, extreme cyclone depth and SLP as well as with the cumulative cyclone presence and
these two measures. Most of the significant observed correlations are reproduced by CESM though
with slightly lower coefficients. The observed correlation between cumulative cyclone presence and
the median radius is not simulated by CESM, while cyclone depth and radius are correlated in CESM
225 but not in the observations.

In summary, CESM is able to realistically simulate cyclones, their extreme characteristics and the
connections among different cyclone characteristics. Some of the discrepancies from ERA interim
can be traced back to the tendency that CESM overestimates the number of weak cyclones.



4 Results

230 4.1 Cyclone intensities during the last millennium

To investigate periods of different cyclonic activity, we define moving averaged indices for all cyclone characteristics, i.e., the cumulative cyclone presence, median of the cyclone radius and the 90th percentile of cyclone depth, SLP, and cyclone-related precipitation (definition see Section 2). First, the indices are estimated for each winter season separately and then averaged over 30-year
235 periods. The resulting time series are shown in Fig. 4.

In the years previous to AD 1850, all indices exhibit strong decadal to multi-decadal variability (Fig. 4). The cumulative cyclone presence shows a clear negative trend after AD 1850 and leaves the preindustrial range around the year 2000. Thus, the CESM projects a lower number of cyclones for the 21st century in the North Atlantic. The geometry illustrated by the median radius of the cyclones
240 remains unaffected by external forcing at a first glance and varies between about 215 to 222 km.

Extreme cyclone depth and central SLP both show a weak trend (positive for cyclone depth and negative for central SLP, but not significant) over the entire time series towards higher wind extremes by the end of the 21st century. They also agree in some of the periods with high intensities, e.g., decades around the years 1300s, 1400s, 1680s, 2060s but around year 2000 extreme SLP indicates its lowest
245 values whereas extreme cyclone depth seems to indicate average years. This difference is a clear indication that it is useful to investigate different intensity measures to conclude on cyclone-related wind extremes. Note that cyclone depth is more related to wind due to the geostrophic approximation compared to SLP which might be influenced by the background pressure (if more cyclones are detected in the low pressure belt they will have deeper central pressure but not necessarily stronger
250 winds).

Extremes in cyclone-related precipitation clearly react to external forcing. Already before 1850, colder periods (17th century and 19th century) which are partly caused by reduced solar and enhanced volcanic forcing show lower than average 90th percentile cyclone-related precipitation whereas warmer periods are associated with higher than average values. Clearly, the warmest period in the simulation is the 21st century and there a strong and significant positive trend is simulated.
255

Some of the new results presented here confirm earlier studies with coarser resolved coupled climate models, e.g., the decrease of cyclone time steps from the preindustrial to the future climate state (e.g., Raible et al., 2007). Still, there are also differences. Raible et al. (2007) suggested a decrease in wind-related intensity from the Maunder Minimum to the present day climate state and attributed this decrease to generally reduced baroclinicity. This is in contrast to the new simulation
260 where no clear sign of an intensification or weakening is found. A major difference between the two analyses is the resolution of the model (in this study around 1°, in Raible et al. (2007) around 4°). Given the high internal variability, as illustrated by the decadal to multi-decadal variations of the two



wind-related indices, the different processes responsible for extreme cyclones (like baroclinicity in
265 the lower and upper troposphere, meridional temperature gradient, diabatic processes) may interplay
differently in the new simulation. At least diabatic processes are better resolved in CESM compared
to the earlier study.

4.2 Natural forcing impact on cyclone characteristics

So far there is no clear sign that natural external forcing (volcanoes and solar variations) has a strong
270 influence on cyclone characteristics whereas at least cyclone-related precipitation shows a strong
trend during the period of strong anthropogenic forcing. To disentangle natural and anthropogenic
forcing impacts we first focus on the potential volcanic and solar influence during the period 850-
1850 CE.

To illustrate the volcanic forcing impact the superposed epoch analysis is applied to the extratropical
275 cyclone characteristics. The 10 strongest volcanic eruptions, according to optical depth anomaly,
over the period 850-1850 CE are composed and time series of the different cyclone characteristics
are presented as deseasonalized monthly anomalies from the 5 years preceding an eruption (simi-
lar to Lehner et al. (2015)). None of the cyclone characteristics show a volcanic forcing influence
(therefore not shown). In particular, wind-related and precipitation-related extremes show no reac-
280 tion after strong volcanic eruptions although the North Atlantic Oscillation tends to be in its positive
phase (Ortega et al., 2015) which has been suggested to be related to wind intense extratropical cy-
clones (Pinto et al., 2009). The missing volcanic forcing impact on precipitation-related extremes
seems to be unexpected as global mean precipitation shows a clear reduction after strong volcanic
eruptions (e.g., Frölicher et al., 2011; Muthers et al., 2014; Lehner et al., 2015). Thus, the results
285 suggest that extremes in both wind and precipitation seems to be decoupled from the mean behavior.

A potential connection between cyclone characteristics and solar variations is investigated by cor-
relating the 30-yr running mean time series (Fig. 4) with the solar forcing (Fig. 1) over the period
850-1850 CE. The analysis with all cyclone characteristics shows that none of the characteristics
have a significant correlation with the solar forcing (the highest correlation coefficient is 0.19 be-
290 tween solar forcing and extreme central pressure). We also tested lag correlations of up to ± 30
years, but again the correlations were not significant at the 5 % level. Thus, a linear connection of
mean and extreme cyclone characteristics to solar forcing is not found in the pre-industrial period of
this simulation.

4.3 Low-frequency variations of extreme cyclone characteristics during the last millennium

295 In the following we will focus on the analysis of the two extreme cyclone characteristics: 90th
percentile of cyclone depth and of cyclone-related precipitation over the North Atlantic region. To
obtain information on the low-frequency of extreme cyclone characteristics, 30-years running aver-



aged periods are investigated in more detail.

Correlation patterns between extreme cyclone depth with different variables like, 2-m temperatures, 300 500-hPa geopotential height, cyclone frequency and mean precipitation show distinct significant (5 % level) patterns in the North Atlantic and over Europe (Fig. 5). Low-frequency variations of extreme cyclone depth correlate negatively with 2-m temperatures around Greenland and positively over Northern and Eastern Europe (Fig. 5a). This correlation is consistent with the correlation found between extreme cyclone depth and 500-hPa geopotential height (Fig. 5b) which resemble 305 a NAO-like structure, but slightly shifted to the north-east, in particular the center located over the Mediterranean Sea. The center north of Iceland is baroclinic, as the corresponding centers of the correlation patterns with the 1000-hPa geopotential height are shifted to the east resulting in a westward tilt with height (not shown). The negative correlations of the 2-m temperature around Greenland go hand in hand with negative correlations between extreme cyclone depth and the sea surface temperature (SST, not shown). This reduction is present over the entire North Atlantic basin, even if 310 the southern part of the Atlantic does not show a statistically significant change. Furthermore, these negative correlations co-occur with positive correlations with sea ice around Iceland (not shown). Additionally, an increase in extreme cyclone depth is related to reduced cyclone frequency and to a reduction of cyclone-related precipitation around Greenland and an increase in both measures 315 around Scandinavia (Fig. 5c,d). Thus, the negative geopotential height anomaly (enhanced low pressure system in the mid of the atmosphere) steers the track of cyclones towards Scandinavia where the cyclone frequency correlates positively with extreme cyclone depth. Furthermore, the correlation pattern of extreme cyclone depth with 2-m temperature show that under increased extreme cyclone depth Scandinavia is located in a region with an enhanced horizontal temperature gradient, and thus 320 a strong baroclinicity. Another important region where low-frequency variations of extreme cyclone depth show significant correlation with other variables is southern Europe. Under high cyclone depth index conditions, it is a region of minimized meridional temperature gradient, as in the north it is relatively warm, while the south, i.e. Africa, is characterized by relatively cold temperatures. Such changes in the temperature field strongly reduce the baroclinic zone, which finally leads to a 325 reduction in cyclone frequency over central Europe and to a reduction in cyclone-related precipitation over southern Europe (Fig. 5c,d, respectively).

Compared to the extreme cyclone depth, which shows distinct and statistically significant correlations, extreme cyclone-related precipitation reveals less clear results. Although an atmospheric wave train can be identified in the correlation pattern of the 500-hPa geopotential height field, it 330 shows no statistical significance over the North Atlantic region (therefore not shown). Although not significant, we find similar patterns in the 1000-hPa geopotential height, indicating that extreme cyclone-related precipitation may be related to barotropic pressure structures. Furthermore, the 2-m temperature reveals a slightly significant positive correlation along the European Atlantic coast (Fig. 6a). Thus, enhanced extreme cyclone-related precipitation is related to a warmer coastal line which



335 leads to increased moisture availability in winter, and thus finally influences the precipitation especially over Iceland, Scandinavia and the Barents Sea (Fig. 6b).

In summary this analysis shows that different circulation and temperature patterns are related to extreme cyclone depth and cyclone-related precipitation. Thus, we can conclude that, on average, cyclones with extreme winds (extreme cyclone depth) are disconnected from cyclones generating
340 extreme precipitation. Nevertheless, this might not be true for single isolated events.

4.4 Anthropogenic forcing impact on cyclone characteristics

Two of the cyclone characteristics (Fig. 4a,e) show strong trends in the 20th and 21st century and thus are influenced by GHG forcing: the cumulative cyclone presence and the cyclone-related precipitation. In contrast, the wind intensity measured by either central pressure or cyclone depth shows no
345 significant trend in the 21st century (Fig. 4c). In the following, we discuss these trends with respect to trends of temperature, precipitation, and cyclone frequency in order to assess potential processes for GHG induced changes in cyclone characteristics. Further, the relevance of thermodynamic processes is investigated by assessing the Clausius-Clapeyron relation.

The temperature trends shown in Fig. 7a are in line with the patterns assessed in IPCC (2013), suggesting a strong warming of the polar areas and the continents and weaker warming of the ocean, in particular the central North Atlantic shows no significant warming. The former is due to polar amplification, induced by a strong sea ice reduction and the reduced heat capacity of the land surface compared to the ocean. The latter is related to changes in the ocean circulation, i.e., a weakening of the AMOC as projected by most of the comprehensive climate models. These different trends
355 lead to a change of the horizontal surface temperature gradients, the latter one is a prerequisite for baroclinicity and thus cyclone development and enhancement. In particular, the contrast between the North Atlantic and Scandinavia is enhanced, a feature also found in the correlation pattern of extreme cyclone depth with temperature in the period 850 to 1850 (Fig. 5). If similar processes worked for decadal variations in the Common Era and the future, we would expect to see a positive trend
360 in extreme cyclone depth, which is not the case in Fig. 4c. Thus, other processes such as increased static stability (Raible et al., 2010) and the overall decreased meridional temperature gradient – both reducing cyclones and wind-related intensity – compensate for the locally increased baroclinicity near Scandinavia.

Precipitation trends also resemble the results presented in the latest IPCC assessment (IPCC, 2013) showing a negative trend over the Mediterranean and a wetting in high latitudes (Fig. 7b). This is a first hint that cyclones are redistributed in the future as most of the precipitation in winter in the mid-latitudes originate from cyclones. Fig. 7c shows the cyclone frequency trend pattern for the 21st century with significant negative trends mainly over the Mediterranean and partly over the central North Atlantic. This pattern resembles the precipitation trends and illustrates the connection between



370 cyclone occurrence and precipitation. As we find a reduction of 12.5 % in the cumulative cyclone
presence over the entire region (Fig. 4a), the reduction over the Mediterranean and the central North
Atlantic cannot be compensated by the positive trends found over Scandinavia and the Hudson Bay
(note that only a small part of the Hudson Bay is included in the area (Fig. 2) of the indices). Again
the signals over the Mediterranean resemble earlier findings obtained with different models (e.g.,
375 Lionello and Giorgi, 2007; Raible et al., 2010). In these studies, enhanced static stability together
with enhanced stationary wave activity are the main reasons for reduced cyclone activity over the
Mediterranean.

The most striking trend of the cyclone characteristics in Fig. 4 is the positive trend of extreme
cyclone-related precipitation in the 20th and 21st century. The trend pattern of temperature (Fig. 7)
380 suggests an overall warming, and thus the capability of the air to hold moisture is strongly increased
in the 21st century. To test whether the trend of extreme cyclone-related precipitation is mainly
due to thermodynamics, we estimate the regression coefficients β between extreme cyclone-related
precipitation and extreme cyclone-related temperature for the entire simulation in a 150-yr running
window and compare them with the range given by the Clausius-Clapeyron relation, i.e., a 2-3 %
385 increase in precipitation per 1°C temperature increase (O’Gorman and Schneider, 2009). Note that
similar results are obtained with a 100-yr running window. The regression coefficients for the period
1851-2100 show a strong shift to the upper bound of the Clausius-Clapeyron relation (3 % increase
in precipitation per 1°C), a level never reached during the Common Era (Fig. 8). This is in line
with recent results of Neelin et al. (2017) who found that the interplay of moisture convergence
390 variance and precipitation loss, increase under global warming. Thus, the result of the 20th and 21st
century agrees with other findings that show that extreme precipitation is mainly thermodynamically
driven, as it follows the Clausius-Clapeyron relation under global warming (e.g., Pall et al.,
2007; O’Gorman and Schneider, 2009; Pendergrass and Gerber, 2016; Neelin et al., 2017). Interest-
ingly, we find that roughly 50 % of the periods in the Common Era show a different behavior where
395 extreme cyclone-related precipitation reacts less to temperature changes than Clausius-Clapeyron
relation would predict, as illustrated by regression coefficients below $(0.16 \text{ mm/day})/^\circ\text{C}$. Thus, we
show that the hypothesized general governance of the Clausius-Clapeyron relation on extreme pre-
cipitation (e.g., Pall et al., 2007; O’Gorman and Schneider, 2009) seems to be time dependent. Hints
that this is not just a model result are found in proxy records over Europe, e.g. flood occurrences
400 cluster also during rather cold periods in the Common Era (e.g., Czymzik et al., 2010; Wirth et al.,
2013; Glur et al., 2013; Amann et al., 2015).

5 Conclusions

Extratropical cyclone characteristics are investigated for the period 850 to 2100 CE in a seamless
transient simulation using CESM (version 1) with the focus on the North Atlantic European region



405 and the winter season (DJF).

The evaluation under present day conditions shows that CESM is able to realistically simulate cyclones and their characteristics, though some biases to the reanalysis product ERA interim remain.

Before 1850, the variability of cyclone characteristics is dominated by internal variability showing pronounced low-frequency variations of different cyclone characteristics. The extreme wind-related characteristics show a significant connection to the large scale dynamics on decadal time scales, whereas the index representing cyclone-related precipitation is only weakly related to the background temperatures on these time scales. The different cyclone characteristics are not correlated with each other over time, being a first indication that external forcing plays no dominant role in generating these variations. A more detailed analysis of the volcanic and the solar forcing imprint confirms this and thus earlier findings with other coarsely resolved climate models (Fischer-Bruns et al., 2005).

Future changes are found in two cyclone characteristics. As only one simulation is used in this study it shows that these changes are pronounced and that we should be able to detect these changes at the beginning to mid of the 21th century, irrespective of the realization of natural variability. The cumulative cyclone presence shows a reduction in the 21st century. This change is already found in studies using coarsely-resolved ensemble simulations with an earlier version of CESM, which compare present day climate with the pre-industrial climate (e.g., Raible et al., 2007). The main decrease of cyclone occurrence is found over the Mediterranean. Using future simulations with another global climate model shows a similar decrease in the Mediterranean (Raible et al., 2010). The process driving the reduction of cyclones over the Mediterranean is the increase in stability and changes in the stationary wave production over the region in winter (Raible et al., 2010). The other characteristic, which shows a dramatic increase in the future, is the extreme cyclone-related precipitation. This increase is driven by the temperature increase and the Clausius-Clapeyron relation, i.e. purely thermodynamically driven. This is in line with a recent study of Neelin et al. (2017). Thus, changes in the dynamics seems to be less important for changing precipitation extremes related to winter cyclone activity in the future.

Extending the analysis of the Clausius-Clapeyron relation back in time reveals prolonged periods in the Common Era where extremes do not follow the Clausius-Clapeyron relation. Thus, we hypothesize that in the Common Era both dynamical and thermodynamical processes can be dominant whereas in the last 100 years and the future under RCP8.5 thermodynamical processes govern extreme events in cyclone-related precipitation. This result is important as many proxy-based studies show that during cold periods of the Common Era hydrological extreme events occur more frequently (Czymzik et al., 2010; Wetter, 2012; Wirth et al., 2013; Glur et al., 2013; Amann et al., 2015). For example, Amann et al. (2015) recently showed in lake sediments that flood occurrences are enhanced during the LIA, a period known to be cold in Europe – a behavior, which cannot be



explained by the Clausius-Clapeyron relation. As the model simulation in this study also shows periods where the Clausius-Clapeyron relation is unable to explain above-normal extreme cyclone precipitation (14th to 15th century) we hypothesize that these periods were dominated by variability of dynamical processes. Moreover, our simulations show that these variations are mainly driven by
445 internal variability and that no systematic response to external forcing like during the LIA is evident. So based on our results, the proxies (e.g. Czymzik et al., 2010; Wetter, 2012; Wirth et al., 2013; Glur et al., 2013; Amann et al., 2015) might just show natural internal variability and hence there is no clear justification to interpret them in context of the LIA (i.e., volcanoes and solar forcing).

Thus, future work shall concentrate on processes of low-frequency changes in cyclone character-
450 istics and the Clausius-Clapeyron relation, e.g., to the assess the role of atmosphere-ocean-sea ice interaction (e.g., Lehner et al., 2013). Further, a more regional view on Europe is needed to focus on impacts on land relevant for insurance providers.

Acknowledgements. This work is supported by the Swiss National Science Foundation (grant: 18-001). The CESM simulation is performed on the super computing architecture of the Swiss National Supercomputing
455 Centre (CSCS).



References

- PAGES 2k Consortium: Ahmed, M., Anchukaitis, K. J., Asrat, A., Borgaonkar, H. P., Braidia, M., Buckley, B. M., Bntgen, U., Chase, B. M., Christie, D. A., Cook, E. R., Curran, M. A. J., Diaz, H. F., Esper, J., Fan, Z.-X., Gaire, N. P., Ge, Q., Gergis, J., Gonzalez-Rouco, J. F., Goosse, H., Grab, S. W., Graham, N., Graham, R., Grosjean, M., Hanhijarvi, S. T., Kaufman, D. S., Kiefer, T., Kimura, K., Korhola, A. A., Krusic, P. J., 460 Lara, A., Lzine, A.-M., Ljungqvist, F. C., Lorrey, A. M., Luterbacher, J., Masson-Delmotte, V., McCarroll, D., McConnell, J. R., McKay, N. P., Morales, M. S., Moy, A. D., Mulvaney, R., Mundo, I. A., Nakatsuka, T., Nash, D. J., Neukom, R., Nicholson, S. E., Oerter, H., Palmer, J. G., Phipps, S. J., Prieto, M. R., Rivera, A., Sano, M., Severi, M., Shanahan, T. M., Shao, X., Shi, F., Sigl, M., Smerdon, J. E., Solomina, O. N., 465 Steig, E. J., Stenni, B., Thamban, M., Trouet, V., Turney, C. S., Umer, M., van Ommen, T., Verschuren, D., Viau, A. E., Villalba, R., Vinther, B. M., von Gunten, L., Wagner, S., Wahl, E. R., Wanner, H., Werner, J. P., White, J. W., Yasue, K., and Zorita, E.: Continental-scale temperature variability during the past two millennia, *Nature Geoscience*, 6, 339–346, doi:10.1038/ngeo1797, 2013.
- Amann, B., Szidat, S., and Grosjean, M.: A millennial-long record of warm season precipitation and flood 470 frequency for the North-western Alps inferred from varved lake sediments: Implications for the future, *Quaternary Science Reviews*, 115, 89–100, doi:10.1016/j.quascirev.2015.03.002, 2015.
- Bengtsson, L., Hodges, K. I., and Roeckner, E.: Storm tracks and climate change, *Journal of Climate*, 19, 3518–3543, doi:10.1175/JCLI3815.1, 2006.
- Bengtsson, L., Hodges, K. I., and Keenlyside, N.: Will extratropical storms intensify in a warmer climate?, 475 *Journal of Climate*, 22, 2276–2301, doi:10.1175/2008JCLI2678.1, 2009.
- Beniston, M.: Linking extreme climate events and economic impacts: Examples from the Swiss Alps, *Energy Policy*, 35, 5384–5392, doi:10.1016/j.enpol.2006.01.032, 2007.
- Björck, S. and Clemmensen, L. B.: Aeolian sediment in raised bog deposits, Halland, SW Sweden: A new proxy record of Holocene winter storminess variation in southern Scandinavia?, *The Holocene*, 14, 677– 480 688, doi:10.1191/0959683604hl746rp, 2004.
- Blender, R., Fraedrich, K., and Lunkeit, F.: Identification of cyclone-track regimes in the North Atlantic, *Quarterly Journal of the Royal Meteorological Society*, 123, 727–741, doi:10.1256/smsqj.53909, 1997.
- Bothe, O., Feng, S., Fernandez-Donado, L., Garcia-Bustamante, E., Gergis, J., Gonzalez-Rouco, F. J., Goosse, H., Hegerl, G., Hind, A., Jungclaus, J., Kaufman, D., Lehner, F., McKay, N., Moberg, A., Raible, C. C., 485 Schurer, A., Smerdon, J., von Gunten, L., Wagner, S., Widmann, M., Yiou, P., and Zorita, E.: Continental scale temperature variability in the PMIP3 simulation ensemble and PAGES 2K regional temperature reconstructions over the past millennium., *Climate of the Past*, 11, 1673–1699, doi:10.5194/cp-11-1673-2015, 2015.
- Braconnot, P., Harrison, S. P., Kageyama, M., Bartlein, P. J., Masson-Delmotte, V., Abe-Ouchi, A., Otto- 490 Bliesner, B., and Zhao, Y.: Evaluation of climate models using palaeoclimatic data, *Nature Climate Change*, 2, 417–424, doi:10.1038/nclimate1456, 2012.
- Bradley, R. S. and Jones, P. D.: 'Little Ice Age' summer temperature variations: Their nature and relevance to recent global warming, *Holocene*, 3, 367–376, 1993.
- Broecker, W. S.: Was a change in thermohaline circulation responsible for the Little Ice Age?, *Proceedings of 495 the National Academy of Sciences*, 97, 1339–1342, doi:10.1073/pnas.97.4.1339, 2000.



- Catto, J. L., Shaffrey, L. C., and Hodges, K. I.: Northern Hemisphere extratropical cyclones in a warming climate in the HiGEM High-Resolution Climate Model, *Journal of Climate*, 24, 5336–5352, doi:10.1175/2011JCLI4181.1, 2011.
- Costas, S., Naughton, F., Goble, R., and Renssen, H.: Windiness spells in SW Europe since the Last Glacial Maximum, *Earth and Planetary Science Letters*, 436, 82–92, doi:10.1016/j.epsl.2015.12.023, 2016.
- Czymzik, M., Dulski, P., Plessen, B., von Grafenstein, U., Naumann, R., and Brauer, A.: A 450 year record of spring-summer flood layers in annually laminated sediments from Lake Ammersee (southern Germany), *Water Resources Research*, 46, doi:10.1029/2009WR008360, w11528, 2010.
- de Jong, R., Schoning, K., and Björck, S.: Increased aeolian activity during humidity shifts as recorded in a raised bog in south-west Sweden during the past 1700 years, *Climate of the Past*, 3, 411–422, doi:10.5194/cp-3-411-2007, 2007.
- Dee, D. P., Uppala, S. M., Simmons, A. J., Berrisford, P., Poli, P., Kobayashi, S., Andrae, U., Balmaseda, M. A., Balsamo, G., Bauer, P., Bechtold, P., Beljaars, A. C. M., van de Berg, L., Bidlot, J., Bormann, N., Delsol, C., Dragani, R., Fuentes, M., Geer, A. J., Haimberger, L., Healy, S. B., Hersbach, H., Hólm, E. V., Isaksen, I., Kållberg, P., Köhler, M., Matricardi, M., McNally, A. P., Monge-Sanz, B. M., Morcrette, J.-J., Park, B.-K., Peubey, C., de Rosnay, P., Tavolato, C., Thépaut, J.-N., and Vitart, F.: The ERA-Interim reanalysis: Configuration and performance of the data assimilation system, *Quarterly Journal of the Royal Meteorological Society*, 137, 553–597, doi:10.1002/qj.828, 2011.
- Degeai, J.-P., Devillers, B., Dezileau, L., Oueslati, H., and Bony, G.: Major storm periods and climate forcing in the Western Mediterranean during the Late Holocene, *Quaternary Science Reviews*, 129, 37–56, doi:10.1016/j.quascirev.2015.10.009, 2015.
- Etienne, C., Goyette, S., and Kuszli, C.-A.: Numerical investigations of extreme winds over Switzerland during 1990–2010 winter storms with the Canadian Regional Climate Model, *Theoretical and Applied Climatology*, 113, 529–547, doi:10.1007/s00704-012-0800-1, 2013.
- Fischer-Bruns, I., Storch, H. v., Gonzalez-Rouco, J. F., and Zorita, E.: Modelling the variability of mid-latitude storm activity on decadal to century time scales, *Climate Dynamics*, 25, 461–476, doi:10.1007/s00382-005-0036-1, 2005.
- Frölicher, T. L., Joos, F., Raible, C. C., and Sarmiento, J. L.: Atmospheric CO₂ response to volcanic eruptions: The role of ENSO, season, and variability, *Global Biogeochem. Cycles*, 27, 239–251, doi:10.1002/gbc.20028, 2011.
- Gagen, M. H., Zorita, E., McCarroll, D., Zahn, M., Young, G. H. F., and Robertson, I.: North Atlantic summer storm tracks over Europe dominated by internal variability over the past millennium, *Nature Geoscience*, 9, 630, doi:10.1038/NGEO2752, 2016.
- Gent, P. R., Danabasoglu, G., Donner, L. J., Holland, M. M., Hunke, E. C., Jayne, S. R., Lawrence, D. M., Neale, R. B., Rasch, P. J., Vertenstein, M., Worley, P. H., Yang, Z.-L., and Zhang, M.: The Community Climate System Model Version 4, *Journal of Climate*, 24, 4973–4991, doi:10.1175/2011JCLI4083.1, 2011.
- Glur, L., Wirth, S. B., Buentgen, U., Gilli, A., Haug, G. H., Schaer, C., Beer, J., and Anselmetti, F. S.: Frequent floods in the European Alps coincide with cooler periods of the past 2500 years, *Scientific Reports*, 3, doi:10.1038/srep02770, 2770, 2013.
- Grieger, J., Leckebusch, G. C., Raible, C. C., Rudeva, I., and Simmonds, I.: Subantarctic cyclones identified



- by 14 tracking methods, and their role for moisture transports into the continent, *Tellus*, 70, doi:10.1080/16000870.2018.1454808, 1454808, 2018.
- Gutowski, W. J., Branscome, L. E., and Stewart, D. A.: Life Cycles of Moist Baroclinic Eddies, *Journal of the Atmospheric Sciences*, 49, 306–319, doi:10.1175/1520-0469(1992)049<0306:LCOMBE>2.0.CO;2, 1992.
- 540 Harvey, B. J., Shaffrey, L. C., Woollings, T. J., Zappa, G., and Hodges, K. I.: How large are projected 21st century storm track changes?, *Geophysical Research Letters*, 39, doi:10.1029/2012GL052873, 118707, 2012.
- Hofer, D., Raible, C. C., Dehnert, A., and Kuhlemann, J.: The impact of different glacial boundary conditions on atmospheric dynamics and precipitation in the North Atlantic region, *Climate of the Past*, 8, 935–949, doi:10.5194/cp-8-935-2012, 2012a.
- 545 Hofer, D., Raible, C. C., Merz, N., Dehnert, A., and Kuhlemann, J.: Simulated winter circulation types in the North Atlantic and European region for preindustrial and glacial conditions, *Geophysical Research Letters*, 39, doi:10.1029/2012GL052296, 2012b.
- Hurrell, J. W., Holland, M. M., Gent, P. R., Ghan, S., Kay, J. E., Kushner, P. J., Lamarque, J.-F., Large, W. G., Lawrence, D., Lindsay, K., Lipscomb, W. H., Long, M. C., Mahowald, N., Marsh, D. R., Neale, R. B.,
550 Rasch, P., Vavrus, S., Vertenstein, M., Bader, D., Collins, W. D., Hack, J. J., Kiehl, J., and Marshall, S.: The Community Earth System Model: A Framework for Collaborative Research, *Bulletin of the American Meteorological Society*, 94, 1339–1360, doi:10.1175/BAMS-D-12-00121.1, 2013.
- IPCC: *Climate Change 2001: The Scientific Basis. Contribution of Working Group I to the Third Assessment Report of the Intergovernmental Panel on Climate Change*, Cambridge University Press, Cambridge, United Kingdom and New York, NY, USA, 2001.
- 555 IPCC: *Climate Change 2013: The Physical Science Basis. Contribution of Working Group I to the Fourth Assessment Report of the Intergovernmental Panel on Climate Change*, Cambridge University Press, Cambridge, United Kingdom and New York, NY, USA, 2013.
- James, I. N. and James, P. M.: Ultra-low-frequency variability in a simple atmospheric circulation model,
560 *Nature*, 342, 53–55, doi:10.1038/342053a0, 1989.
- Kidston, J., Vallis, G. K., Dean, S. M., and Renwick, J. A.: Can the increase in the eddy length scale under global warming cause the poleward shift of the jet streams?, *Journal of Climate*, 24, 3764–3780, doi:10.1175/2010JCLI3738.1, 2011.
- Laine, A., Kageyama, M., Salas-Melia, D., Voltaire, A., Riviere, G., Ramstein, G., Planton, S., Tyteca, S.,
565 and Peterschmitt, J. Y.: Northern hemisphere storm tracks during the last glacial maximum in the PMIP2 ocean-atmosphere coupled models: Energetic study, seasonal cycle, precipitation, *Climate Dynamics*, 32, 593–614, doi:10.1007/s00382-008-0391-9, 2009.
- Lehner, F., Born, A., Raible, C. C., and Stocker, T. F.: Amplified inception of European Little Ice Age by sea ice-ocean-atmosphere feedbacks, *Journal of Climate*, 26, 7586–7602, doi:10.1175/JCLI-D-12-00690.1,
570 2013.
- Lehner, F., Joos, F., Raible, C. C., Mignot, J., Born, A., Keller, K. M., and Stocker, T. F.: Climate and carbon cycle dynamics in a CESM simulation from 850 to 2100 CE, *Earth System Dynamics*, 6, 411–434, doi:10.5194/esd-6-411-2015, 2015.
- Li, M., Woollings, T., Hodges, K., and Masato, G.: Extratropical cyclones in a warmer, moister climate: A
575 recent Atlantic analogue, *Geophysical Research Letters*, 41, 8594–8601, doi:10.1002/2014GL062186, 2014.



- Lionello, P. and Giorgi, F.: Winter precipitation and cyclones in the Mediterranean region: Future climate scenarios in a regional simulation, *Adv Geo Sci*, 12, 153–158, 2007.
- Lionello, P., Trigo, I. F., Gil, V., Liberato, M. L. R., Nissen, K., Pinto, J. G., Raible, C. C., Reale, M., Tanzarella, A., Trigo, R. M., Ulbrich, S., and Ulbrich, U.: Objective climatology of cyclones in the Mediterranean region: A consensus view among methods with different system identification and tracking criteria, *Tellus*, 68, doi:10.3402/tellusa.v68.29391, 29391, 2016.
- 580 McDonald, R. E.: Understanding the impact of climate change on Northern Hemisphere extra-tropical cyclones, *Climate Dynamics*, 37, 1399–1425, doi:10.1007/s00382-010-0916-x, 2011.
- McGregor, H. V., Evans, M. N., Goosse, H., Leduc, G., Martrat, B., Addison, J. A., Mortyn, P. G., Oppo, D. W., Seidenkrantz, M. S., Sicre, M. A., Phipps, S. J., Selvaraj, K., Thirumalai, K., Filipsson, H. L., and V. E.: Robust global ocean cooling trend for the pre-industrial Common Era, *Nature Geoscience*, 8, 671677, doi:10.1038/NGEO2510, 2015.
- 585 Merz, N., Raible, C. C., and Woollings, T.: North Atlantic eddy-driven jet in interglacial and glacial winter climates, *Journal of Climate*, 28, 3977–3997, doi:10.1175/JCLI-D-14-00525.1, 2015.
- 590 Muthers, S., Anet, J. G., Raible, C. C., Brönnimann, S., Rozanov, E., Arfeuille, F., Peter, T., Shapiro, A. I., Beer, J., Steinhilber, F., Brugnara, Y., and Schmutz, W.: Northern hemispheric winter warming pattern after tropical volcanic eruptions: Sensitivity to the ozone climatology, *Journal of Geophysical Research*, 110, 1340–1355, doi:10.1002/2013JD020138, 2014.
- Neelin, J. D., Sahany, S., Stechmann, S. N., and Bernsteina, D. N.: Global warming precipitation accumulation increases above the current-climate cutoff scale, *Proceedings of the National Academy of Sciences*, 114, 1258–1263, doi:10.1073/pnas.1615333114, 2017.
- 595 Neu, U., Akperov, M. G., Bellenbaum, N., Benestad, R., Blender, R., Caballero, R., Cocozza, A., Dacre, H. F., Feng, Y., Fraedrich, K., Grieger, J., Gulev, S., Hanley, J., Hewson, T., Inatsu, M., Keay, K., Kew, S. F., Kindem, I., Leckebusch, G. C., Liberato, M. L. R., Lionello, P., Mokhov, I. I., Pinto, J. G., Raible, C. C., Reale, M., Rudeva, I., Schuster, M., Simmonds, I., Sinclair, M., Sprenger, M., Tilinina, N. D., Trigo, I. F., Ulbrich, S., Ulbrich, U., Wang, X. L., and Wernli, H.: IMILAST: A community effort to intercompare extratropical cyclone detection and tracking algorithms, *Bulletin of the American Meteorological Society*, 94, 529–547, doi:10.1175/BAMS-D-11-00154.1, 2013.
- 600 O’Gorman, P. A.: Understanding the varied response of the extratropical storm tracks to climate change, *Proceedings of the National Academy of Sciences*, 107, 19 176–19 180, doi:10.1073/pnas.1011547107, 2010.
- O’Gorman, P. A. and Schneider, T.: Energy of midlatitude transient eddies in idealized simulations of changed climates, *Journal of Climate*, 21, 5797–5806, doi:10.1175/2008JCLI2099.1, 2008.
- O’Gorman, P. A. and Schneider, T.: The physical basis for increases in precipitation extremes in simulations of 21st-century climate change, *Proceedings of the National Academy of Sciences*, 106, 14 773–14 777, doi:10.1073/pnas.0907610106, 2009.
- 610 Ortega, P., Lehner, F., Swingedouw, D., Masson-Delmotte, V., Raible, C. C., Casado, M., and Yiou, P.: A model-tested North Atlantic Oscillation reconstruction for the last millennium, *Nature*, 523, 71–75, doi:10.1038/nature14518, 2015.
- Otto-Bliessner, B. L., Brady, E. C., J. F., Jahn, A., Landrum, L., Stevenson, S., Rosenbloom, N., Mai, A., and G. S.: Climate variability and change since 850 CE: An ensemble approach with the Community Earth System
- 615



- Model, *Bulletin of the American Meteorological Society*, 99, 735–754, 2016.
- Pall, P., Allen, M., and Stone, D.: Testing the Clausius-Clapeyron constraint on changes in extreme precipitation under CO₂ warming, *Climate Dynamics*, 28, 351–363, doi:10.1007/s00382-006-0180-2, 2007.
- Pendergrass, A. G. and Gerber, E. P.: The rain is askew: Two idealized models relating vertical velocity and precipitation distributions in a warming world, *J. Climate*, 29, 6445–6462, doi:10.1175/JCLI-D-16-0097.1, 2016.
- Pinto, J., Karremann, M., Born, K., Della-Marta, P., and Klawa, M.: Loss potentials associated with European windstorms under future climate conditions, *Climate Research*, 54, 1–20, doi:10.3354/cr01111, 2012.
- Pinto, J. G., Zacharias, S., Fink, A. H., Leckebusch, G. C., and Ulbrich, U.: Factors contributing to the development of extreme North Atlantic cyclones and their relationship with the NAO, *Climate Dynamics*, 32, 711–737, doi:10.1007/s00382-008-0396-4, 2009.
- Rahmstorf, S., Box, J. E., Feulner, G., Mann, M. E., Robinson, A., Rutherford, S., and Schaffernicht, E. J.: Exceptional twentieth-century slowdown in Atlantic Ocean overturning circulation, *Nature Climate Change*, 5, 475–480, doi:10.1038/NCLIMATE2554, 2015.
- 630 Raible, C. C.: On the relation between extremes of midlatitude cyclones and the atmospheric circulation using ERA40, *Geophysical Research Letters*, 34, doi:10.1029/2006GL029084, 107703, 2007.
- Raible, C. C. and Blender, R.: Midlatitude cyclonic variability in GCM-simulations with different ocean representations, *Climate Dynamics*, 22, 239–248, doi:10.1007/s00382-003-0380-y, 2004.
- Raible, C. C., Yoshimori, M., Stocker, T. F., and Casty, C.: Extreme midlatitude cyclones and their implications to precipitation and wind speed extremes in simulations of the Maunder Minimum versus present day conditions, *Climate Dynamics*, 28, 409–423, doi:10.1007/s00382-006-0188-7, 2007.
- 635 Raible, C. C., Della-Marta, P., Schwierz, C., Wernli, H., and Blender, R.: Northern Hemisphere extratropical Cyclones: A Comparison of Detection and Tracking Methods and different Re-analyses, *Monthly Weather Review*, 136, 880–897, doi:10.1175/2007MWR2143.1, 2008.
- 640 Raible, C. C., Ziv, B., Saaroni, H., and Wild, M.: Winter synoptic-scale variability over the Mediterranean Basin under future climate conditions as simulated by the ECHAM5, *Climate Dynamics*, 35, 473–488, doi:10.1007/s00382-009-0678-5, 2010.
- Riviere, G.: A dynamical interpretation of the poleward shift of the jet streams in global warming scenarios, *Journal of the Atmospheric Sciences*, 68, 1253–1272, doi:10.1175/2011JAS3641.1, 2011.
- 645 Sabatier, P., Dezileau, L., Colin, C., Briquieu, L., Bouchette, F., Martinez, P., Siani, G., Raynal, O., and Von Grafenstein, U.: 7000-years of paleostorm activity in the NW Mediterranean Sea in response to Holocene climate events, *Quaternary Research*, 77, 1–11, doi:10.1016/j.yqres.2011.09.002, 2012.
- Schiesser, H. H., Pfister, C., and Bader, J.: Winter storms in Switzerland North of the Alps 1864/1865–1993/1994, *Theoretical and Applied Climatology*, 58, 1–19, doi:10.1007/BF00867428, 1997.
- 650 Schmidt, G. A., Jungclaus, J. H., Ammann, C. M., Bard, E., Braconnot, P., Crowley, T. J., Delaygue, G., Joos, F., Krivova, N. A., Muscheler, R., Otto-Bliesner, B. L., Pongratz, J., Shindell, D. T., Solanki, S. K., Steinhilber, F., and Vieira, L. E. A.: Climate forcing reconstructions for use in PMIP simulations of the last millennium (v1.0), *Geoscientific Model Development*, 4, 33–45, doi:10.5194/gmd-4-33-2011, 2011.
- Schneider, T., O’Gorman, P. A., and Levine, X. J.: Water vapor and the dynamics of climatic changes, *Reviews of Geophysics*, 48, doi:10.1029/2009RG000302, 2010.
- 655



- Schneidereit, A., Blender, R., and Fraedrich, K.: A radius - depth model for midlatitude cyclones in reanalysis data and simulations, *Quarterly Journal of the Royal Meteorological Society*, 136, 50–60, doi:10.1002/qj.523, 2010.
- Smerdon, J. E., Luterbacher, J., Phipps, S. J., Anchukaitis, K. J., Ault, T., Coats, S., Cobb, K. M., Cook, B. I., Colose, C., Felis, T., Gallant, A., Jungclaus, J. H., Konecky, B., LeGrande, A., Lewis, S., Lopatka, A. S., Man, W. M., Mankin, J. S., Maxwell, J. T., Otto-Bliesner, B. L., Partin, J. W., Singh, D., Steiger, N. J., Stevenson, S., Tierney, J. E., Zanchettin, D., Zhang, H., Atwood, A. R., Andreu-Hayles, L., Baek, S. H., Buckley, B., Cook, E. R., D'Arrigo, R., Dee, S. G., Griffiths, M. L., Kulkarni, C., Kushnir, Y., Lehner, F., Leland, C., Linderholm, H. W., Okazaki, A., Palmer, J., Piovano, E., Raible, C. C., Rao, M. P., Scheff, J., Schmidt, G. A., Seager, R., Widmann, M., Williams, A. P., and Xoplaki, E.: Comparing proxy and model estimates of hydroclimate variability and change over the Common Era, *Climate of the Past*, 13, 1851–1900, doi:10.5194/cp-13-1851-2017, 2017.
- Taylor, K. E., Stouffer, R. J., and Meehl, G. A.: An overview of CMIP5 and the experiment design, *Bulletin of the American Meteorological Society*, 93, 485498, doi:10.1175/BAMS-D-11-00094.1, 2012.
- Trouet, V., Scourse, J., and Raible, C.: North Atlantic storminess and Atlantic Meridional Overturning Circulation during the last Millennium: Reconciling contradictory proxy records of NAO variability, *Global and Planetary Change*, 84–85, 48–55, doi:10.1016/j.gloplacha.2011.10.003, 2012.
- Ulbrich, U., Pinto, J. G., Kupfer, H., Leckebusch, G. C., Spanghel, T., and Reyers, M.: Changing northern hemisphere storm tracks in an ensemble of IPCC climate change simulations, *Journal of Climate*, 21, 1669–1679, doi:10.1175/2007JCLI1992.1, 2008.
- Van Vliet-Lanoe, B., Penaud, A., Henaff, A., Delacourt, C., Fernane, A., Goslin, J., Hallegouet, B., and Le Cornec, E.: Middle- to late-Holocene storminess in Brittany (NW France): Part II - The chronology of events and climate forcing, *The Holocene*, 24, 434–453, doi:10.1177/0959683613519688, 2014.
- Wetter, O.: Hochwasser Katastrophen in Basel vom 13. bis 21. Jahrhundert: Rekonstruktion, Deutung und Lerneffekte, in: *Krisen Crises. Ursachen, Deutungen, Folgen.*, vol. 27, Schweizerisches Jahrbuch für Wirtschafts- und Sozialgeschichte, 48–63, 2012.
- Willison, J., Robinson, W. A., and Lackmann, G. M.: The importance of resolving mesoscale latent heating in the North Atlantic storm track, *Journal of the Atmospheric Sciences*, 70, 2234–2250, doi:10.1175/JAS-D-12-0226.1, 2013.
- Wirth, S. B., Gilli, A., Simonneau, A., Ariztegui, D., Vanniere, B., Glur, L., Chapron, E., Magny, M., and Anselmetti, F. S.: A 2000 year long seasonal record of floods in the southern European Alps, *Geophysical Research Letters*, 40, 4025–4029, doi:10.1002/grl.50741, 2013.
- Woollings, T., Gregory, J. M., Pinto, J. G., Reyers, M., and Brayshaw, D. J.: Response of the North Atlantic storm track to climate change shaped by oceanatmosphere coupling, *Nature Geoscience*, 5, 313–317, doi:10.1038/ngeo1438, 2012a.
- Woollings, T., Harvey, B., Zahn, M., and Shaffrey, L.: On the role of the ocean in projected atmospheric stability changes in the Atlantic polar low region, *Geophysical Research Letters*, 39, doi:10.1029/2012GL054016, l24802, 2012b.
- Woollings, T., Franzke, C., Hodson, D. L. R., Dong, B., Barnes, E. A., Raible, C. C., and Pinto, J. G.: Contrasting interannual and multidecadal NAO variability, *Climate Dynamics*, 45, 539–556, doi:10.1007/



s00382-014-2237-y, 2015.

Zalasiewicz, J., Williams, M., Steffen, W., and Crutzen, P.: The New World of the Anthropocene, *Environmental Science & Technology*, 44, 2228–2231, doi:10.1021/es903118j, 2010.

700 Zappa, G., Shaffrey, L. C., Hodges, K. I., Sansom, P. G., and Stephenson, D. B.: A multimodel assessment of future projections of North Atlantic and European extratropical cyclones in the CMIP5 climate models, *Journal of Climate*, 26, 5846–5862, doi:10.1175/JCLI-D-12-00573.1, 2013.

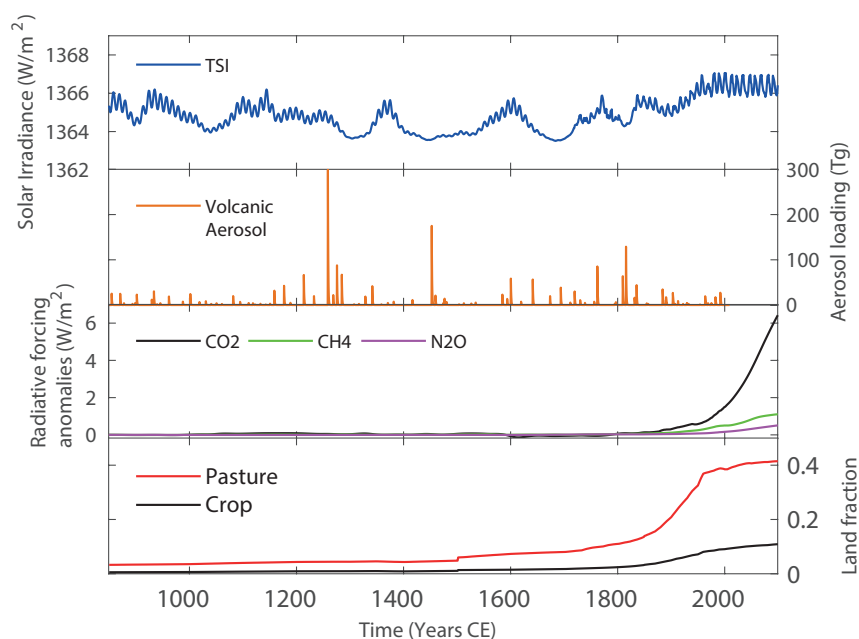


Fig. 1. Forcings used in the last millennium simulation with CESM. From Top to bottom: total solar irradiance (TSI), total volcanic aerosol mass; radiative forcing (calculated according to IPCC, 2001) from the greenhouse gases CO₂, CH₄, and N₂O; and major changes in land cover as fraction of global land area. The figure is adapted from Lehner et al. (2015).

Table 1. Correlation between different cyclone characteristics. The upper right of the table represent CESM correlation, the lower left ERA interim. Bold numbers indicate significant correlation at the 5 % level using a two-side student *T* test. For this analysis the central SLP time series is multiplied by -1 so that low central pressure corresponds to a high cyclone depth resulting in a positive correlation.

	Cyclone time steps	Radius	Cyclone depth	SLP	Cyclone rel. Precipitation
cyclone time steps	1	0.21	-0.42	-0.49	0.11
Radius	0.42	1	0.47	-0.36	0.07
Cyclone depth	-0.4	0.09	1	0.63	0.16
SLP	-0.58	0.07	0.81	1	0.13
Cyclone rel. Precipitation	-0.27	-0.11	0.22	0.15	1

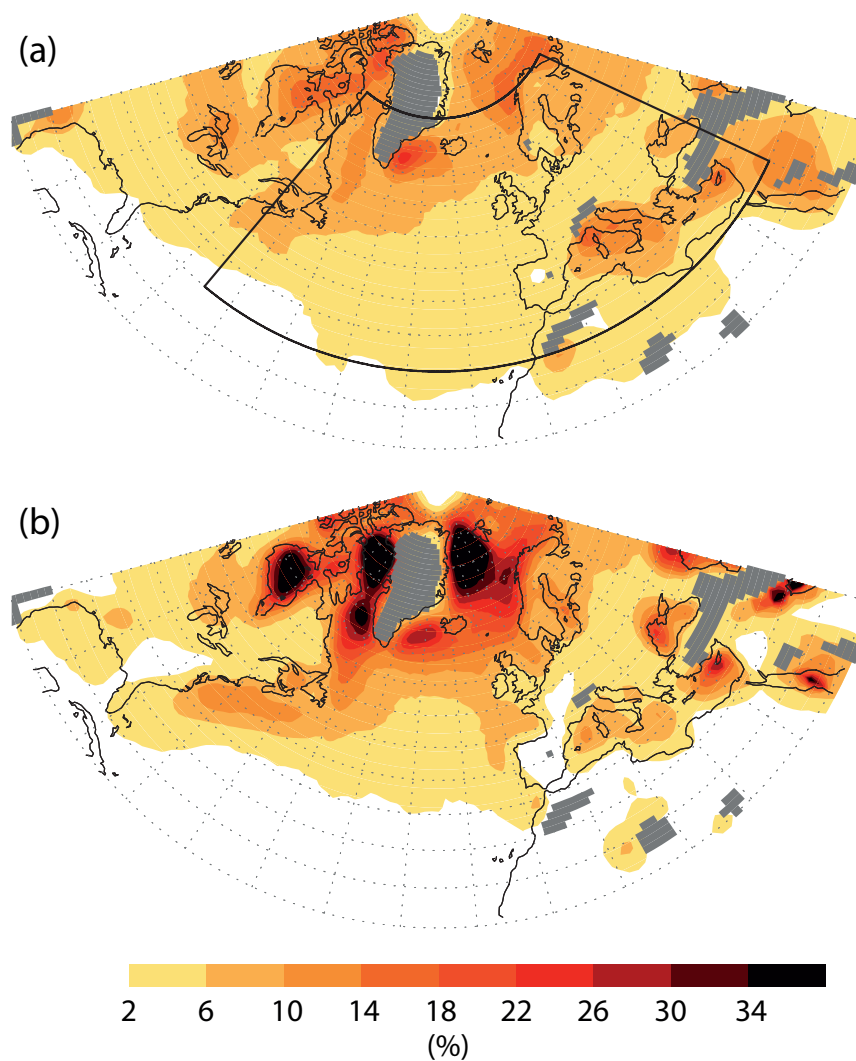


Fig. 2. Cyclone center frequency (% presence per season) for (a) the ERA interim and (b) the CESM simulation for the period AD 1980-2009 in winter (DJF). The bounded domain illustrates the region North Atlantic used to estimate different cyclone characteristics. Grey areas are higher than 1 km above sea level and are excluded from the cyclone detection and tracking method. 10% presence per season means that in 10% of the winter season a cyclone is present at a grid point.

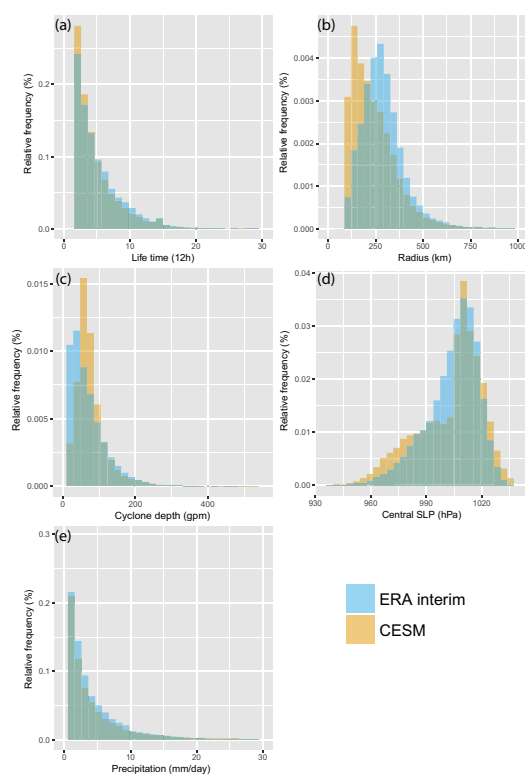


Fig. 3. Histograms of different cyclone characteristics: (a) life time of cyclones, (b) radius of cyclones, and (c) cyclone depth, (d) central SLP and (e) cyclone-related precipitation. The histograms are based on the cyclones detected from 1981-2010, i.e., 7624 cyclones in ERA interim and 12369 in CESM.

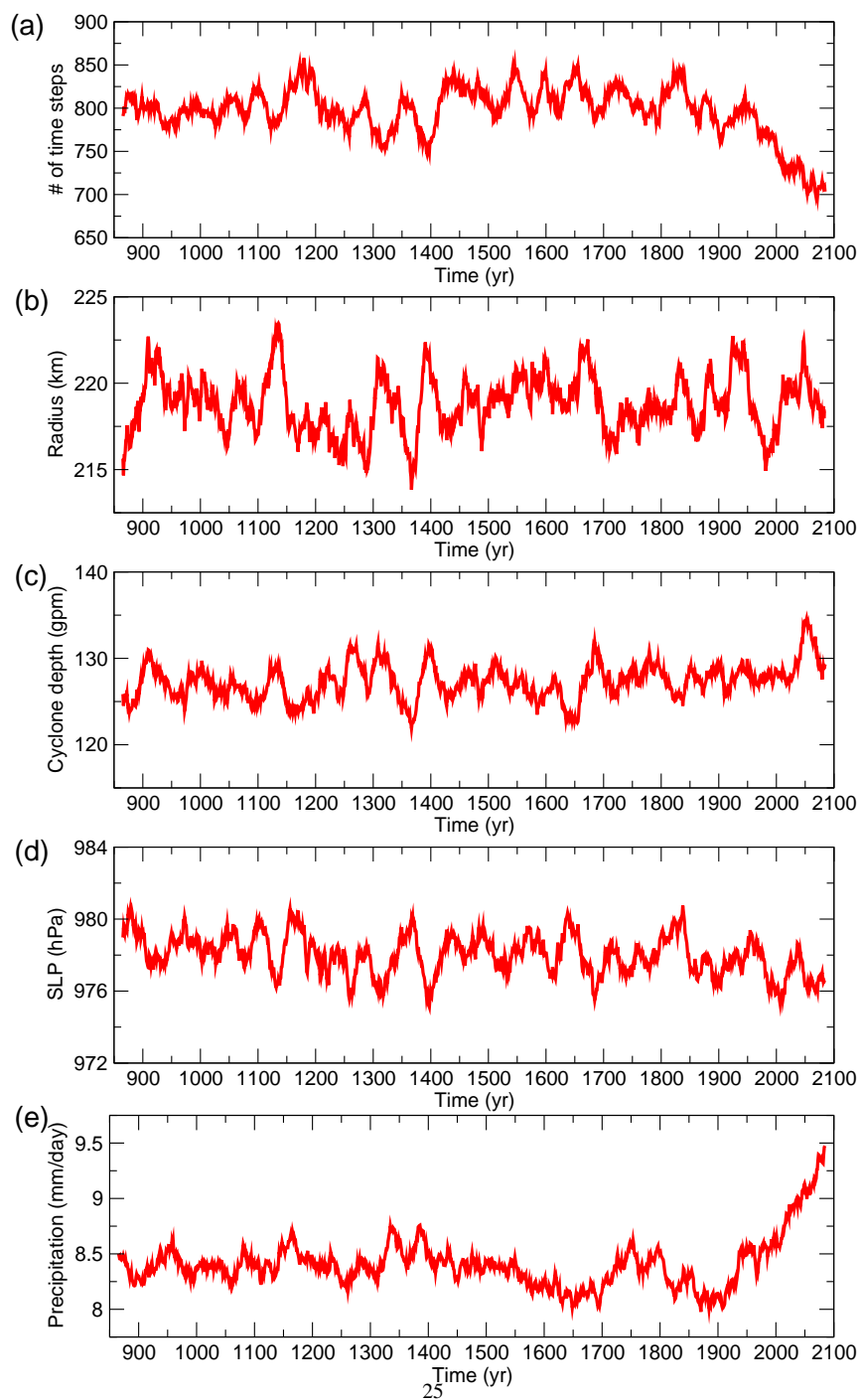


Fig. 4. Long-term time behavior of different cyclone characteristics illustrated by time series averaged with 30-yr running window: (a) cumulative cyclone presence, (b) median radius of the cyclones, and 90th percentile of (c) cyclone depth, (d) central SLP and (e) cyclone-related precipitation.

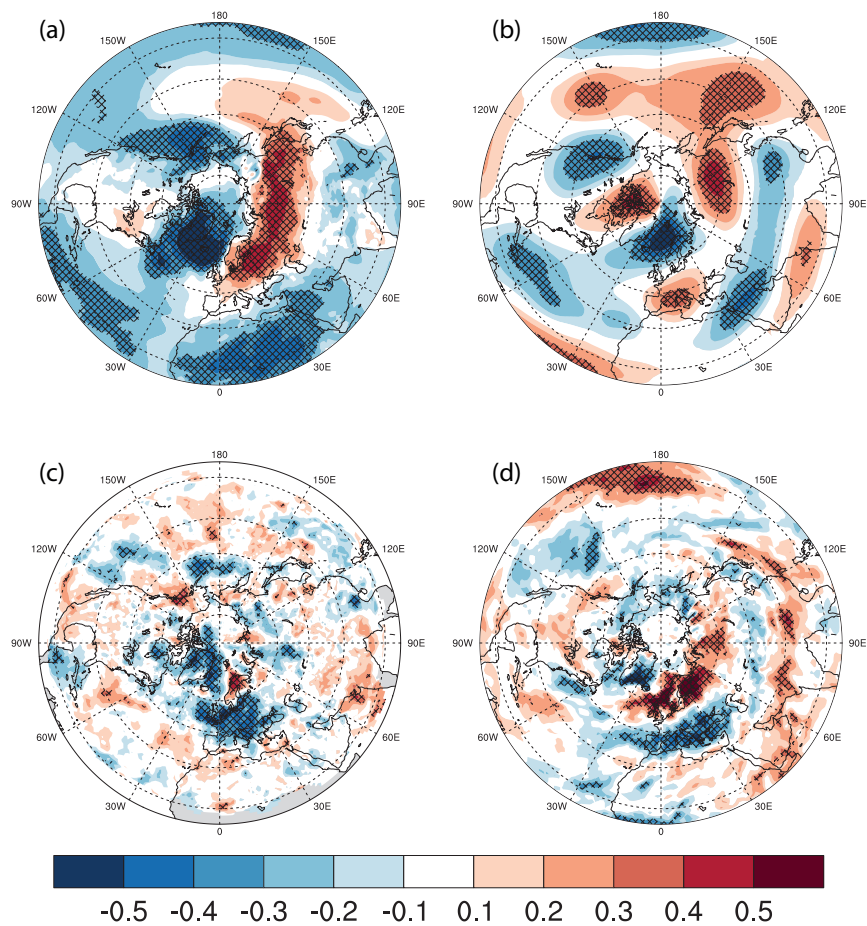


Fig. 5. Correlation between the 30-yr running mean times series of extreme cyclone depth and (a) 2-m temperature, (b) 500-hPa geopotential height, (c) cyclone frequency, and (d) precipitation for the period 850-1850 CE. The 5 % significance level using a student *T*-test is illustrated with cross-hatching.

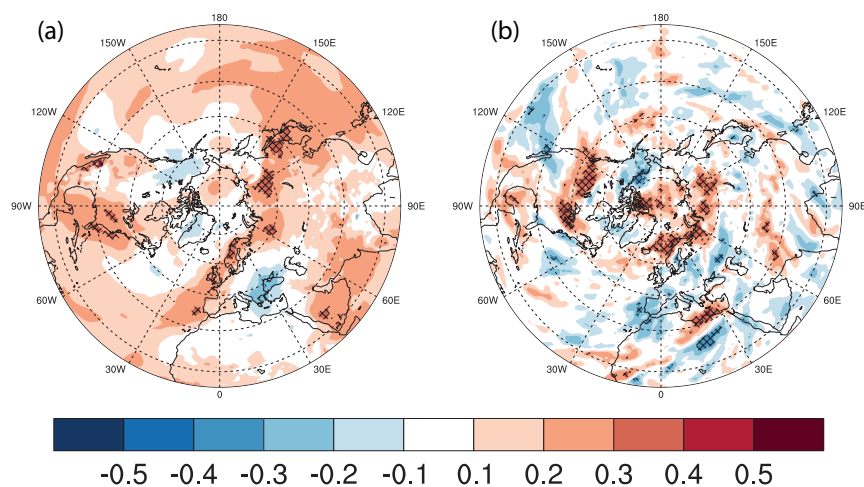


Fig. 6. Correlation between the 30-yr running mean times series of extreme cyclone-related precipitation and (a) 2-m temperature and (b) precipitation for the period 850-1850 CE. The 5% significance level using a student *T*-test is illustrated with cross-hatching.

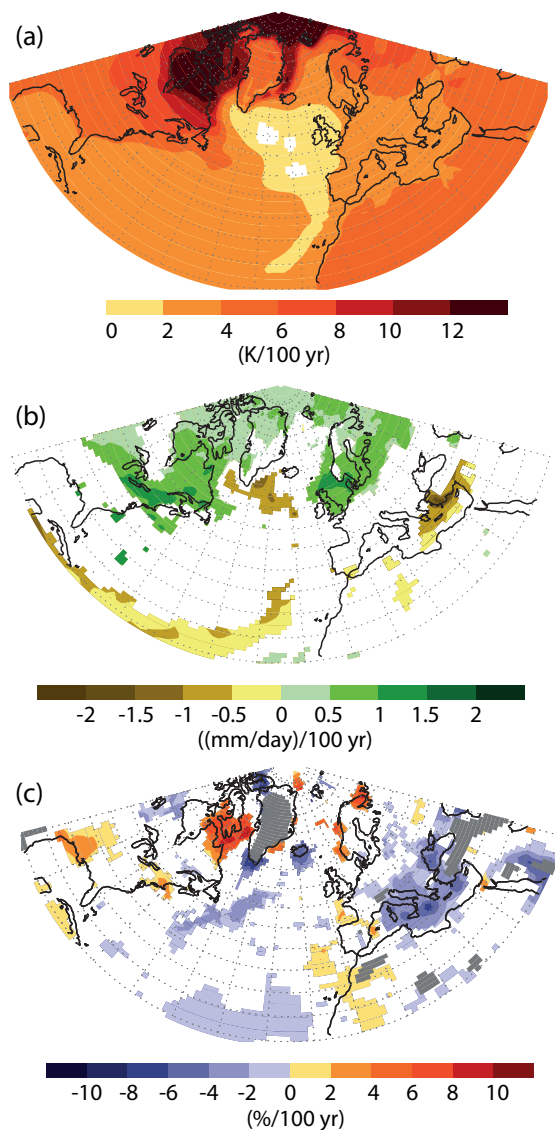


Fig. 7. Trends from 2005 to 2100 for (a) 2-m temperature, (b) precipitation, and (c) cyclone frequency. Only significant trends at the 5 % significance level using a student T -test are shaded. Grey areas in (c) are excluded from the cyclone detection and tracking method (1000 m a.s.l.).

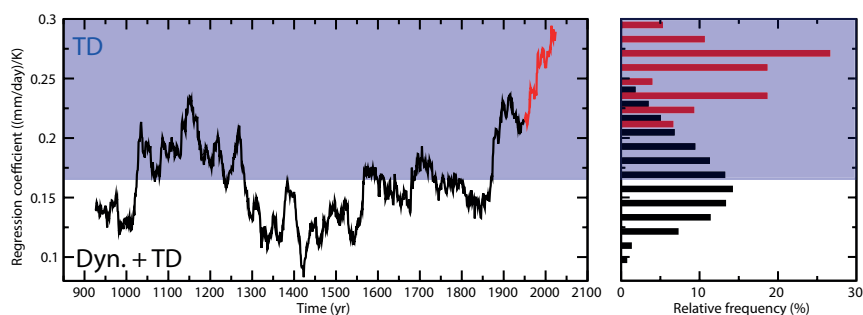


Fig. 8. Time series of regression coefficient estimated between mean cyclone-related temperature and 90th percentile of cyclone-related precipitation for 150-yr window running through the entire period 850 to 2100: Common Era (black) and era influenced by RPC8.5 (red). The right panel shows the histogram of the regression coefficients for the two periods (bin width 0.01). All periods within the blue shading follow the Clausius-Clapeyron relation, named thermodynamic (TD) (O’Gorman and Schneider, 2009). In the white area, dynamics (Dyn.) and thermodynamics are relevant.